

# Hand Preference and Sex Shape the Architecture of Language Networks

Patric Hagmann,<sup>1,2\*</sup> Leila Cammoun,<sup>1</sup> Roberto Martuzzi,<sup>2</sup>  
Philippe Maeder,<sup>2</sup> Stephanie Clarke,<sup>3</sup> Jean-Philippe Thiran,<sup>1</sup>  
and Reto Meuli<sup>2</sup>

<sup>1</sup>Signal Processing Institute, Ecole Polytechnique Fédérale de Lausanne (EPFL), Lausanne, Switzerland

<sup>2</sup>Department of Radiology, University Hospital, Lausanne, Switzerland

<sup>3</sup>Division of Neuropsychology, University Hospital, Lausanne, Switzerland

**Abstract:** In right-handed subjects, language processing relies predominantly on left hemisphere networks, more so in men than in women, and in right- versus left-handers. Using DT-MRI tractography, we have shown that right-handed men are massively interconnected between the left-hemisphere language areas, whereas the homologous in the right hemisphere are sparse; interhemispheric connections between the language areas and their contralateral homologues are relatively strong. Women and left-handed men have equally strong intrahemispheric connections in both hemispheres, but women have a higher density of interhemispheric connections. *Hum Brain Mapp* 27:828–835, 2006. © 2006 Wiley-Liss, Inc.

**Key words:** language; sex; hand preference; handedness; connectivity; DTI; diffusion MRI; tractography; fibertracking; Broca; Wernicke; brain asymmetry; accurate fasciculus; corpus callosum

## INTRODUCTION

Language comprehension and production rely critically on left hemispheric networks, including Broca's area, which contributes to language production and is located in the opercular part of the inferior frontal gyrus (oIFG), and Wernicke's area, which contributes to language comprehension and is located in the planum temporale and the posterior part of the superior temporal gyrus [pSTG; Dronkers et al., 2004; Gernsbacher and Kaschak, 2003; Martin, 2003]. Activation studies suggest that left hemispheric dominance for

language processing is less strong in women than in men [Jaeger et al., 1998; Shaywitz et al., 1995] and in left-handed (LH) than in right-handed (RH) individuals [Pujol et al., 1999; Tzourio et al., 1998]. Matching the functional asymmetry, Broca's [Falzi et al., 1982; Foundas et al., 1996] and to a certain degree in Wernicke's areas [e.g., Foundas et al., 1994; Galaburda et al., 1978; Steinmetz et al., 1989; but see also Josse et al., 2003; Shapleske et al., 1999] were found to be larger on the left side. Sex and handedness seem to influence the degree of anatomical asymmetry; in Wernicke's area the asymmetry was reported to be smaller in LH than in RH [Foundas et al., 2002; Moffat et al., 1998; Steinmetz et al., 1991] and in women than in men [Good et al., 2001].

Relatively little is known about the organization of language areas. They are believed to be part of a widespread neural network, but only small parts of its connectivity have been demonstrated anatomically [Di Virgilio et al., 1999]. The intrinsic organization of language areas has been investigated histologically. The morphology of the main cortical output neurons, the pyramids [Jacobs et al., 1993; Seldon, 1985], and the spacing of long-range intrinsic connections [Galuske et al., 2000] were found to be somewhat different

Contract grant sponsor: Swiss National Science Foundation (SNSF); Contract grant sponsor: Yves Paternot.

\*Correspondence to: Patric Hagmann, Signal Processing Institute, Ecole Polytechnique Fédérale de Lausanne (EPFL), Lausanne 1015, Vaud, Switzerland. E-mail: patric.hagmann@epfl.ch

Received for publication 16 February 2005; Revised 13 June 2005, 5 October 2005; Accepted 17 October 2005

DOI: 10.1002/hbm.20224

Published online 15 March 2006 in Wiley InterScience (www.interscience.wiley.com).

between Wernicke's area and its right homologue. Broca's area was found to have a greater neuronal density than its homologue, especially in men [Amunts et al., 1999]. These differences are likely to be accompanied by differences in long distance connectivity, although this has never been systematically investigated.

We report here on the connectivity of Broca's and Wernicke's areas and their right hemisphere homologues, as visualized with DT-MRI tractography [Hagmann et al., 2003] in RH and LH men and women. Taking advantage of the strong relation between axonal orientation and water diffusion, DT-MRI fibertracking is a technique that allows the visualization of water diffusion coherence lines in brain tissue and consequently is a unique technique to map axonal trajectories in vivo and noninvasively [Mori and van Zijl, 2002]. These computer-generated lines commonly are referred to as virtual fibers. When the tractography method is run in the whole brain, by generating fibers uniformly the number of virtual fibers, if normalized appropriately between two regions, can be seen as a measure of connection density as it captures the tract size and its diffusion coherence. Furthermore the fiber tract volume on its own can be studied.

## PATIENTS AND METHODS

We investigated 32 subjects (16 men, 8 RH and 8 LH; mean age  $\pm$  standard deviation [SD],  $34.0 \pm 7.9$  years; and 16 women, 8 RH and 8 LH; mean age  $\pm$  SD,  $29.2 \pm 6.2$  years). Handedness was defined according to the Edinburgh-Oldfield inventory [Oldfield, 1971], ranging from  $-10$  to  $+10$ , with positive and negative scores representing RH and LH, respectively. Mean handedness score and SD for the respective groups were: RH women =  $9.4 \pm 1.2$ , RH men =  $7.0 \pm 2.1$ , LH women =  $-6.5 \pm 3.2$  and LH men =  $-6.4 \pm 2.6$ . This research was conducted in agreement with the Code of Ethics of the World Medical Association (Declaration of Helsinki) and informed consent was obtained from all subjects before performing the study, in accordance with institutional guidelines.

For each of the 32 subjects, we acquired at 1.5 T:

1. Two functional magnetic resonance imaging (fMRI) studies with a single-shot gradient-echo echo-planar imaging (EPI) sequence (repetition time [TR] = 15 seconds for the sentence comprehension task and 5 seconds for the word generation task, 16 slices, slice thickness 5 mm, gap 1 mm, echo time [TE] = 66 msec, field of view [FoV] =  $270 \times 270$  mm<sup>2</sup>, matrix size  $128 \times 128$ , flip angle 90 degrees);
2. A DT-MRI dataset based on a single-shot EPI sequence (TR/TE = 1,000/89 msec, 44 contiguous slices of 3-mm thickness, FoV =  $210 \times 210$  mm<sup>2</sup>, matrix size  $128 \times 128$ ) acquired at b-value = 1,000 sec/mm<sup>2</sup> along six diffusion-sensitizing directions placed with a sagittal symmetry and forming the vertices of an icosahedron [Jones, 2004]; and
3. A sagittal T1-weighted 3D gradient-echo sequence (128

contiguous slices, slice thickness 1.25 mm, FoV =  $250 \times 250$  mm<sup>2</sup>, matrix size  $256 \times 256$ ).

The two fMRI studies consisted of a sentence-comprehension paradigm (subjects were asked to detect errors while listening to a random sequence of grammatically correct or incorrect sentences), and in a silent word-generation paradigm. Both studies were organized according to a block design. These two functional studies were used to map in each subject areas related to language processing, and in particular pSTG and oIFG. Functional MRI data analysis was carried out with SPM2 (The Wellcome Department of Cognitive Neurology, London, UK).

DT-MRI datasets were used as input for a fibertracking method [Hagmann et al., 2003]. The solutions of this tracking algorithm are a set of lines or virtual fiber trajectories. Each line is the result of a random walk in a diffusion tensor field. This walk, indexed by a time-dependent position vector  $q_i$ , is driven by the local diffusion properties, i.e., the diffusion tensor  $D_i$ , and a regularity constraint vector  $\Omega_{i-1}$  to ensure smooth trajectories. More precisely we have

$$q_{i+1} = q_i + \mu \Omega_i. \quad (1)$$

The displacement of size  $\mu = 1$  mm at each step occurs along direction  $\Omega_i$  that is defined as:

$$\Omega_i = \begin{cases} \lambda d_i + \Omega_{i-1} \\ \|\lambda d_i + \Omega_{i-1}\| \\ \Omega_i \cdot \Omega_{i-1} > 0 \end{cases} \quad (2)$$

where  $d_i = \|D_i^\alpha r_i\|^{-1} D_i^\alpha r_i$ , with  $r_i$  a random vector uniformly distributed over the sphere. The random anisotropic diffusion is modeled by  $d_i$  and  $\Omega_{i-1}$ , the previous displacement, serves as a regularity constraint.  $\Omega_i \cdot \Omega_{i-1} > 0$  ensures a forward propagation only;  $\alpha$  was set to 3 and  $\lambda$  to 1. A detailed discussion of the effect of the various parameters can be found in Hagmann et al. [2003]. Such fibers were initiated extensively and uniformly over all the brain white matter (for every cube of  $2 \times 2 \times 2$  mm<sup>3</sup> there were 15 initializations) and grown until they reached the white matter mask boundary. This mask is defined by thresholding fractional anisotropy (FA) map at 0.2. A threshold set at 0.2 seems optimal to separate gray from white matter, as on average white matter has a FA of over 0.3 and gray matter of 0.1–0.15. The large set of fibers (several hundred thousands) thus generated provides an estimate of axonal trajectories throughout the brain.

For each subject, the fibertracts of interest were selected through a pair of regions of interest (ROIs; Fig. 1), which in this study were based on the individual fMRI activations. The four local maxima in the  $t$ -score activation maps of the corresponding language comprehension and production fMRIs were identified automatically and named target points. They gave us for every subject the position of the center of left and right pSTG and oIFG. In a few cases, where

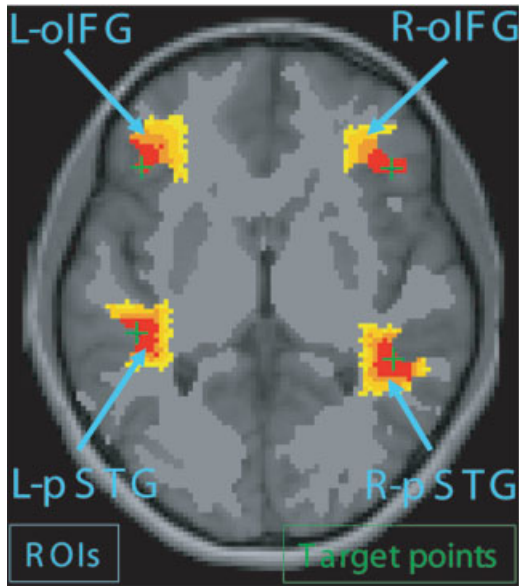


**Figure 1.**

Schema of the fMRI-located ROIs. The green crosses represent the target points, which are identified by the local maximum of the related fMRI activation. The red-to-yellow regions define the ROIs that have been generated by a geodesic region-growing algorithm; all 4 ROIs have the same volume.

there was no right oIFG activation, the target point was placed according to the contralateral activation and placed in the homologous cortical location. Among the eight subjects in each group we had three RH women, four RH men, three LH women, and four LH men who had no significant activation in the left oIFG and consequently needed manual placement.

From each of these four target points we grew a ROI by an iterative procedure that adds at each step one layer of voxel to the current ROI under the constraint that the ROI cannot grow outside the mask and must have a specified final volume that was chosen to be  $8.82 \text{ cm}^3$  (Fig. 1). The particularity of this algorithm is to create geodesic ROIs with shapes that follow local white matter configuration and of strictly equal white matter volume for all ROIs and all subjects. Furthermore, in this procedure, human intervention is very limited as the target points are defined with an objective fMRI criterion and the ROIs automatically defined by the algorithm. The fiber selection was done by retaining the fibers that had one extremity in each chosen ROI. In this manner, only the anatomical connectivity between the functional areas under investigation is measured and the other pathways discarded.

From the computed fibers between two ROIs, the tract volume could also be calculated by counting the number of voxels that had at least one fiber passing through; this result was then multiplied by the voxel volume.

White matter volume  $V_{\text{WM}}$  was estimated by measuring the volume of the fibertracking mask (the fractional anisot-

ropy map thresholded at 0.2). The midsagittal callosal surface  $S_{\text{CC}}$  was measured in the midsagittal plane of the same mask. As we will see further down, the data are measures of limited range in the sense that their values extend between  $-1$  and  $+1$  or between  $0$  and plus infinity; therefore, the statistics were always carried out on log-transformed data to remove skewness. We used either a one-way or two-way analysis of variance (ANOVA) test with a significance threshold for null hypothesis rejection set to  $\alpha = 0.05$ .

## RESULTS

Using the method described above, we visualized by DT-MRI tractography the axonal connectivity between Wernicke's and Broca's areas and their right hemisphere homologues, i.e., between left and right pSTG and oIFG (Fig. 2).

### Intrahemispheric Connectivity

The intrahemispheric connections between pSTG and oIFG formed a loose bundle that we call the pSTG–oIFG bundle, which was very reminiscent of the arcuate fasciculus revealed by tracing studies in nonhuman primates [Petrides and Pandya, 1988].

In many but not all subjects, the pSTG–oIFG bundle tended to have more fibers on the left than on the right side. Connective lateralization index was defined as:  $cLI = \log[(1 + Q)/(1 - Q)]$ , which is the Fisher Z-transform of the quotient  $Q = (N_L - N_R)/(N_L + N_R)$ ,  $N$  being the number of fibers that run between pSTG and oIFG, left (L) and right (R). A positive value for  $cLI$  means a lateralization toward the left (i.e., the pSTG–oIFG connectivity is stronger left than right); negative values mean the opposite, and zero means ambilaterality. By means of this measure, we investigated the effect of handedness and sex on the lateralization of the pSTG–oIFG bundle. One-way ANOVA showed that RH men were significantly more lateralized than LH men toward the left ( $F[1,14] = 6.9504$ ,  $P < 0.05$ ).

Women presented little asymmetry in the pSTG–oIFG connection density, which was not statistically significant between RH and LH ( $F[1,14] = 0.5545$ ,  $P > 0.05$ ). Two-way ANOVA combining handedness and sex showed a significant interaction between both effects ( $F[1,28] = 6.5561$ ,  $P < 0.05$ ; Fig. 3).

The same study was repeated by replacing the fiber count ( $N$ ) by the tract volume ( $V$ ). Accordingly,  $Q$  is rewritten as  $Q = (V_L - V_R)/(V_L + V_R)$ . The statistical analysis yielded analogous results. In terms of tract volume, RH men were significantly more lateralized toward the left than LH men ( $F[1,14] = 11.9555$ ,  $P < 0.005$ ), whereas women were not ( $F[1,14] = 2.6666$ ,  $P > 0.05$ ). Handedness and sex interaction proved to be highly significant on a two-way ANOVA ( $F[1,28] = 13.8943$ ,  $P < 0.005$ ).

The size of the pSTG–oIFG bundle was compared between subjects after normalization with respect to the total white matter volume. We define the normalized connection density  $A$  as  $nCD_A = \log[\gamma N/V_{\text{WM}}]$ , which is the log transform of the number of fibers that run between two ipsilateral

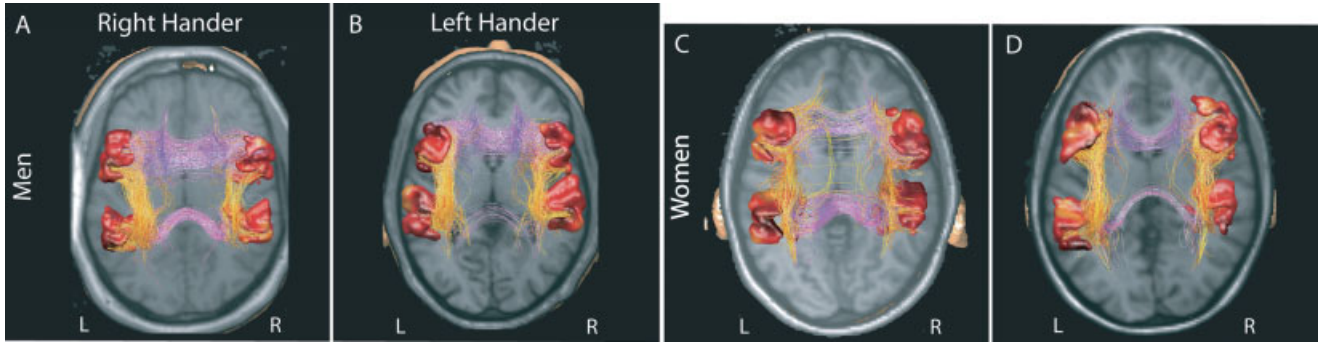


**Figure 2.**

Intra- and interhemispheric white matter connections between language areas. Superior view of a T1-weighted axial MRI slice. The red surfaces mark the cortical gray matter adjacent to the 4 ROIs located in the left and right pSTG and oIFG. These ROIs, of identical white matter volume, have been generated by a geodesic region-growing algorithm so that they follow the brain conformation. They are initialized at the local maximum of the fMRI activations related to language comprehension or production (see Patients and Methods). Yellow-red denotes intrahemispheric connections; magenta-blue denotes interhemispheric. The latter

crossed in the body of the corpus callosum when linking both oIFG, or in the isthmus for the pSTG. **A:** RH men typically presented a marked asymmetry in the pSTG–oIFG bundle, with more fibers in the left hemisphere. Posterior interhemispheric connections were numerous. **B:** LH men typically presented little asymmetry in the pSTG–oIFG bundle. The posterior interhemispheric connections were sparse. RH (**C**) and LH (**D**) women had similar connectivity patterns; i.e., both had a strong intra- and interhemispheric connectivity.

ROIs (N), normalized by the total white matter volume ( $V_{WM}$ ). And  $V_{WM}$  is proportional to the total number of fibers.  $\gamma = 500$  is a constant value, identical for all groups, that is chosen for having distributions of  $nCD_A$  and the associated boxplot gathered around 0. The effect of handedness and hemisphere was assessed with a two-way ANOVA by computing the  $nCD_A$  of left and right pSTG–oIFG bundles in RH and LH. Men exhibited a statistically significant handedness effect ( $F[1,28] = 5.3066$ ,  $P < 0.05$ ) as well as interaction ( $F[1,28] = 5.4562$ ,  $P < 0.05$ ), shown in Figure 4. When the same analysis was done removing the outlier visible in Figure 4, the handedness effect vanishes ( $F[1,27] = 4.0105$ ,  $P = 0.055$ ) in favor of a stronger interaction effect ( $F[1,27] = 8.6092$ ,  $P = 0.0067$ ).

The same analysis done with the tract volumes ( $\log[\text{tract volume}]$ ) confirms these results. We observed a similar strong interaction effect ( $F[1,28] = 7.9791$ ,  $P = 0.0086$ ), whereas handedness ( $F[1,28] = 0.61243$ ,  $P > 0.05$ ) and hemisphere ( $F[1,28] = 1.0972$ ,  $P > 0.05$ ) effects were not significant.

These observations demonstrate that RH and LH men exhibit clear different intrahemispheric connectivity patterns. Although the RH men clearly exhibit a smaller right than left bundle, it seems also that LH men generally have a more symmetric and high connection density with a potential tendency to a reversed asymmetry, as demonstrated by the strong interaction. No such effects were visible in the group of women (Fig. 4).

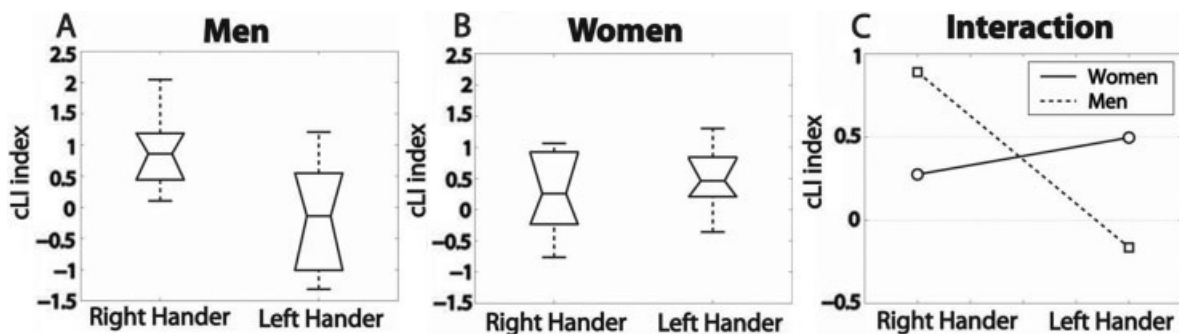


**Figure 3.**

Lateralization of the pSTG–oIFG bundle, i.e., respective density of connections as measured by the cLI index; box plot, and interaction plot. **A:** RH men are significantly more lateralized than LH men toward the left hemisphere. **B:** RH women cannot be differentiated from LH women. **C:** Significant interaction between sex and handedness.

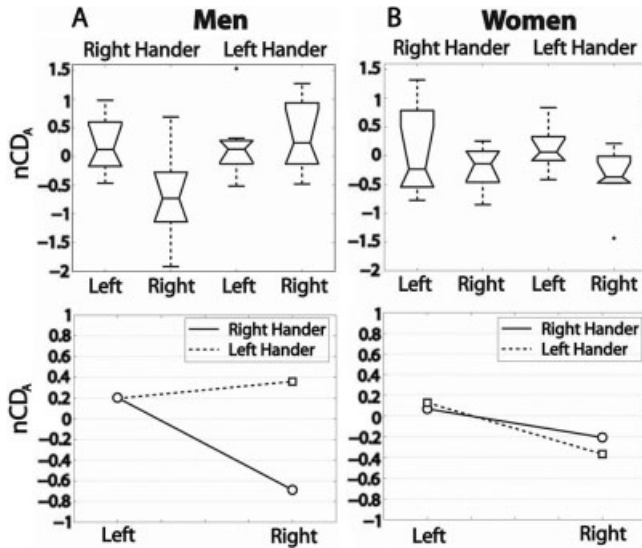


**Figure 4.**

Connection density of the pSTG–oIFG bundle measured by the  $nCD_A$  index, box plots, and interaction plot. Left and Right refer to the hemisphere. **A:** Among men there is a significant handedness effect combined with an interaction between side and handedness that is due to a small right bundle in right handers. **B:** Neither handedness nor side effects is significant in women.

### Interhemispheric Connectivity

Interhemispheric connections between the left and right pSTG formed a relatively loose bundle and crossed the midsagittal plane at the level of the isthmus and anterior splenium; those between the left and right oIFG crossed at the level of the body of the corpus callosum (Fig. 2). For interindividual comparison, we used a log transform of the number of fibers ( $N$ ) that run between left and right pSTG or left and right oIFG normalized by callosal surface ( $nCD_B = \log[\gamma N / S_{CC}]$ ) to account for the putative relation between the midsagittal callosal area versus handedness and sex [Luders et al., 2003]. Again,  $\gamma = 10$  is a constant to gather the distributions around 0.

Figure 5A displays the interhemispheric oIFG connections that did not present any significant effect in terms of handedness or sex. Stronger variation was present for the pSTG interhemispheric connectivity (Fig. 5). In particular, sex ( $F[1,28] = 9.3247$ ,  $P < 0.005$ ) and handedness ( $F[1,28] = 5.8583$ ,  $P < 0.05$ ) effects of a two-way ANOVA were statistically significant in the sense that female sex and RH effects favor posterior interhemispheric connectivity. A striking difference was the sparseness of interhemispheric pSTG connections in LH men (Fig. 5B).

Again, tract volumetric analysis exhibited compatible results. Practically, the number of fibers ( $N$ ) was replaced by the tract volume ( $V$ ) in the  $nCD_B$  formula ( $\log[\gamma V / S_{CC}]$ ). Although inter-oIFG volumetry did not show any significant results, inter-pSTG volumetry yielded significant sex

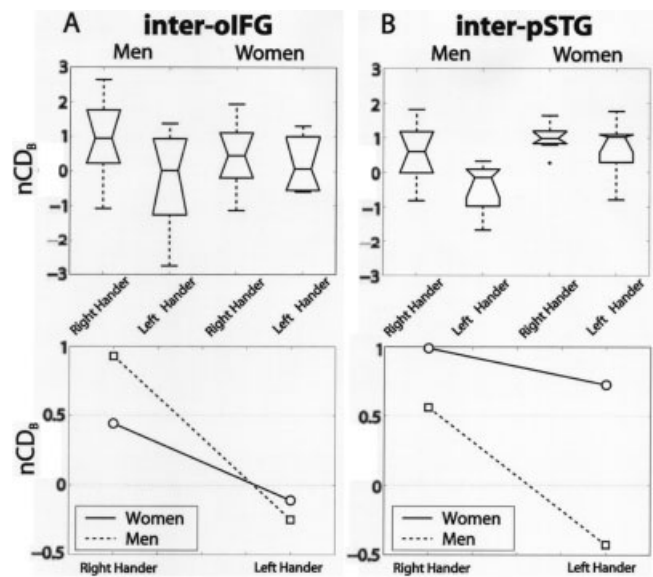
( $F[1,28] = 7.9682$ ,  $P < 0.05$ ) and handedness ( $F[1,28] = 6.3716$ ,  $P < 0.05$ ) effects of a two-way ANOVA.

Figure 6 displays in volumetric units the distributions of the tract volumes grouped according to sex, handedness, and tract type.

We also tested the same hypotheses as on connection densities and tract volume on the average tract FA. Interestingly, no hypothesis was statistically significant using average FA.

### DISCUSSION

Before discussing the above results, we need to take into account the possible limitation of our investigation method that are of different kind. First, we need to remember that we measure water diffusion and that the computed tractography lines are only interpreted as fiber tracts [Beaulieu, 2002]. Accordingly, there is a statistical uncertainty in the tract solutions. This probabilistic relationship between axonal model and diffusion measurements is taken into account inherently by our tractography method at the price of a potential decrease of sensitivity compared with standard streamline algorithm [Mori and van Zijl, 2002]. Second, the arcuate fasciculus travels through the centrum semi-ovale, a region that is well known for its crossing structures [Haggmann et al., 2004]; DT-MRI badly resolves such partial volume effects. Accordingly, the connection density might be underestimated but this in similar extents in both hemispheres. Much care has been taken to avoid biasing the



**Figure 5.**

Interhemispheric connectivity ( $nCD_B$ ), box plots, and interaction plots (see Interhemispheric Connectivity). **A:** Inter-oIFG connection density does not show any difference between men and women, RH and LH. **B:** Inter-pSTG connection density exhibits a significant handedness and sex effect. The connections of the LH men are particularly sparse.

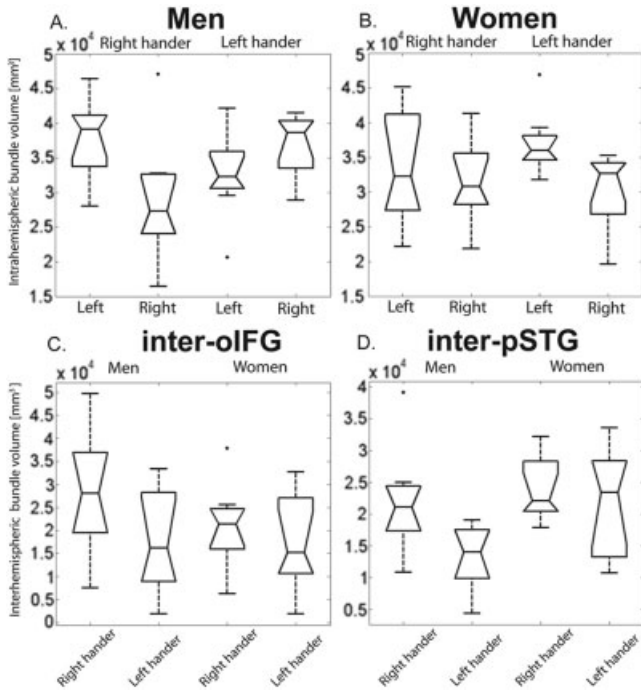


**Figure 6.**

Tract volumes according to the different groups. Volume ( $\text{mm}^3$ ) of the left and right pSTG–olFG bundles in LH and RH men (A) and women (B). C: Volume ( $\text{mm}^3$ ) of the inter-olFG bundles in men and women and in RH and LH. D: Volume ( $\text{mm}^3$ ) of the inter-pSTG bundle in men versus women and in RH versus LH.

results. Although not totally optimal, the six-directional sagittally symmetric icosahedral diffusion signal sampling scheme we used [Jones, 2004], the well-fixed and centered head placement, and the fMRI-based ROI center identification with automatic ROI generation by algorithmic region growing should be sufficient to limit potential bias in interhemispheric comparison studies. Finally, tractography on its own is not sufficient to claim the existence of new yet not described fiber tracts, as the technique is subjects to many artifacts. It is therefore important that such tracing studies are hypothesis driven and based on complementary data such as postmortem investigations. Despite these limitations, diffusion MRI-based fibertracking is becoming a well-recognized tool for neuroanatomical connectivity investigation of macroscopic structures. In particular, several studies have shown that an accurate measurement of the arcuate fasciculus is possible with DT-MRI [Catani et al., 2005; Hagmann et al., 2003; Mori et al., 2002]. In this particular study, we used two complementary measurement approaches: connection density (or normalized fiber counting) and tract volumetry. Both methods yielded very similar statistics, thus strengthening the results. The fact that the statistics of tract volumetry were strongly related to the connection density whereas average tract FA seemed not to exhibit any specific pattern raises an interesting remark. Based on what we know from the relation between diffusion pattern and

underlying axonal organization [Beaulieu, 2002; von dem Hagen and Henkelman, 2002], it seems that the differences measured between the different groups comes more from the tract size than from the tract compactness or axonal regular alignment.

Direct connections between Wernicke's and Broca's areas as well as between Broca's or Wernicke's area and their homologue have been postulated based on postmortem tracing studies in nonhuman primates [Petrides and Pandya, 1988]. Based on this hypothesis, we have found in RH men stronger connections between Wernicke's and Broca's areas than between their homologues in the right hemisphere. The existence of structural asymmetry of Wernicke's and Broca's areas is debated. Size as well as shape asymmetries have been described [Foundas et al., 1998; Good et al., 2001; Josse et al., 2003]. This asymmetry in the density of intrahemispheric connectivity, however, is supported by circumstantial evidence from cytoarchitectonic studies. Large pyramidal neurons, which are a putative source of long association connections, were found to be more numerous in Broca's [Hayes and Lewis, 1995] and Wernicke's areas [Hutsler, 2003] than in their homologues in the right hemisphere. This is in agreement with our data and with previous diffusion MRI studies, which demonstrated greater diffusion tensor anisotropy [Buchel et al., 2004; Cao et al., 2003] as well as greater connectivity [Parker et al., 2005] in the region of the left arcuate fasciculus in populations constituted predominantly by RH men.

Strong interconnectivity has been often described between areas belonging to the same functional system, such as the dorsal or ventral streams in vision [Ungerleider and Haxby, 1994]. Strong interconnectivity between Wernicke's and Broca's areas thus confirms the existence of an integrated language network, as suggested already by reports of frequent coactivation of these areas in a variety of language tasks [Gernsbacher and Kaschak, 2003].

Women and LH men tended to have equally strong intrahemispheric connections between Wernicke's and Broca's areas as between their homologues, suggesting an extension of the integrated language network to the right hemisphere. Such an interpretation is supported by activation studies, which showed that language tasks yielded more right hemisphere activation in LH men [Tzourio et al., 1998] or groups of women and LH men [Pujol et al., 1999] than in RH men. The tendency toward functional similarity of Broca's and Wernicke's areas and their homologues is also reflected in the lesser anatomical asymmetry reported in left-handed individuals [Foundas et al., 2002; Moffat et al., 1998; Steinmetz et al., 1991].

Language networks that are confined to a single (left) hemisphere or distributed over the two hemispheres are likely to require different amounts of interhemispheric connectivity. The exclusively left hemisphere network needs to have access to information that is received and processed initially in the right hemisphere, such as sensory information concerning the left auditory and visual hemisphere or the left hand. In agreement with this, Wernicke's and Broca's

areas have been shown to receive homotopic (the present work) and heterotopic interhemispheric connections [Di Virgilio et al., 1999].

The bihemispheric network needs connections between language areas on either side, and possibly connections from nonlanguage areas in one hemisphere to the language areas in the other hemisphere. The amount of interhemispheric connectivity required by an exclusively left hemisphere network versus bihemispheric network has been estimated differently by different authors. Based on tracing experiments in male rats, Buchel et al [2004] postulated that increased asymmetry of a region is accompanied by a smaller density of interhemispheric connections. In humans, such a relationship was proposed for Wernicke's area based on circumstantial evidence: the part of the corpus callosum in which the fibers from Wernicke's area were believed to cross [isthmus; Aboitiz et al., 1992] was smaller in subjects with greater asymmetry and within this callosal part, there were fewer small diameter axons, the origin and termination of which were not known [Zaidel et al., 1995]. Further but controversial support came from studies of left-handers, who tend to have less asymmetrical language areas: a few studies reported a larger posterior corpus callosum in LH than in RH individuals, although more numerous studies denied it [for review see Beaton, 1997]. A recent, very thorough anatomical MRI study concluded that the relationship between cerebral asymmetries and callosal size and shape is far from clear [Luders et al., 2003].

Our results suggest that callosal connectivity of less asymmetrical language areas is implemented differently in men than it is in women. Language comprehension area-related callosal connections tended to be less dense in LH than in RH men. This goes against the rat model of hemispheric asymmetry and callosal connectivity [Galaburda et al., 1990] and does not fit the circumstantial evidence from human studies. The latter used global measures of callosal subparts [Aboitiz et al., 1992] or axonal density of unknown origin [Zaidel et al., 1995], whereas we have visualized callosal connections belonging specifically to language areas. The intense callosal connectivity in RH men thus may be the support for a strong functional coordination between both areas [Tzourio-Mazoyer et al., 2004], whereas the more bihemispherically distributed language network in LH men seems to require less callosal connectivity. The latter may rely on higher levels of language-related processing within the right hemisphere, so that callosal connections of the language areas convey only information concerning the highest levels of language processing and do not provide transfer of basic information.

In comparison to RH men, RH and LH women tend to be less lateralized for language [Jaeger et al., 1998; Shaywitz et al., 1995]. The density of their language-related callosal connections, however, is similar to that of RH men and there is no measurable difference in this respect between RH and LH women. Their more bihemispherically distributed language network seems to be organized differently than that in LH men, with notably more dense interhemispheric connections.

These differences in callosal connectivity between less-lateralized language networks in women and in LH men may be the result of differential axonal elimination and maturation during development [Innocenti, 1994; Schmithorst et al., 2002], which is probably influenced by hormonal regulation [Morris et al., 2004].

## ACKNOWLEDGMENTS

We thank Prof. Stefan Morgenthaler and Prof. Peter Clarke for their useful comments.

## REFERENCES

- Aboitiz F, Scheibel AB, Zaidel E (1992): Morphometry of the Sylvian fissure and the corpus callosum, with emphasis on sex differences. *Brain* 115:1521–1541.
- Amunts K, Schleicher A, Burgel U, Mohlberg H, Uylings HB, Zilles K (1999): Broca's region revisited: cytoarchitecture and intersubject variability. *J Comp Neurol* 412:319–341.
- Beaton AA (1997): The relation of planum temporale asymmetry and morphology of the corpus callosum to handedness, gender, and dyslexia: a review of the evidence. *Brain Lang* 60:255–322.
- Beaulieu C (2002): The basis of anisotropic water diffusion in the nervous system—a technical review. *NMR Biomed* 15:435–455.
- Buchel C, Raedler T, Sommer M, Sach M, Weiller C, Koch MA (2004): White matter asymmetry in the human brain: a diffusion tensor MRI study. *Cereb Cortex* 14:945–951.
- Cao Y, Whalen S, Huang J, Berger KL, DeLano MC (2003): Asymmetry of subinsular anisotropy by in vivo diffusion tensor imaging. *Hum Brain Mapp* 20:82–90.
- Catani M, Jones DK, ffytche DH (2005): Perisylvian language networks of the human brain. *Ann Neurol* 57:8–16.
- Di Virgilio G, Clarke S, Pizzolato G, Schaffner T (1999): Cortical regions contributing to the anterior commissure in man. *Exp Brain Res* 124:1–7.
- Dronkers NF, Wilkins DP, Van Valin RD Jr, Redfern BB, Jaeger JJ (2004): Lesion analysis of the brain areas involved in language comprehension. *Cognition* 92:145–177.
- Falzi G, Perrone P, Vignolo LA (1982): Right-left asymmetry in anterior speech region. *Arch Neurol* 39:239–240.
- Foundas AL, Eure KF, Luevano LF, Weinberger DR (1998): MRI asymmetries of Broca's area: the pars triangularis and pars opercularis. *Brain Lang* 64:282–296.
- Foundas AL, Leonard CM, Gilmore R, Fennell E, Heilman KM (1994): Planum temporale asymmetry and language dominance. *Neuropsychologia* 32:1225–1231.
- Foundas AL, Leonard CM, Gilmore RL, Fennell EB, Heilman KM (1996): Pars triangularis asymmetry and language dominance. *Proc Natl Acad Sci USA* 93:719–722.
- Foundas AL, Leonard CM, Hanna-Pladdy B (2002): Variability in the anatomy of the planum temporale and posterior ascending ramus: do right- and left handers differ? *Brain Lang* 83:403–424.
- Galaburda AM, LeMay M, Kemper TL, Geschwind N (1978): Right-left asymmetries in the brain. *Science* 199:852–856.
- Galaburda AM, Rosen GD, Sherman GF (1990): Individual variability in cortical organization: its relationship to brain laterality and implications to function. *Neuropsychologia* 28:529–546.
- Galuske RA, Schlote W, Bratzke H, Singer W (2000): Interhemispheric asymmetries of the modular structure in human temporal cortex. *Science* 289:1946–1949.

- Gernsbacher MA, Kaschak MP (2003): Neuroimaging studies of language production and comprehension. *Annu Rev Psychol* 54:91–114.
- Good CD, Johnsrude I, Ashburner J, Henson RN, Friston KJ, Frackowiak RS (2001): Cerebral asymmetry and the effects of sex and handedness on brain structure: a voxel-based morphometric analysis of 465 normal adult human brains. *Neuroimage* 14:685–700.
- Hagmann P, Reese T, Tseng W, Meuli R, Thiran J, Wedeen V (2004): Diffusion spectrum imaging tractography in complex cerebral white matter: an investigation of the centrum semiovale. *Proc Intl Soc Mag Reson Med* 11:623.
- Hagmann P, Thiran JP, Jonasson L, Vandergheynst P, Clarke S, Maeder P, Meuli R (2003): DTI mapping of human brain connectivity: statistical fiber tracking and virtual dissection. *Neuroimage* 19:545–554.
- Hayes TL, Lewis DA (1995): Anatomical specialization of the anterior motor speech area: hemispheric differences in magnopyramidal neurons. *Brain Lang* 49:289–308.
- Hutsler JJ (2003): The specialized structure of human language cortex: pyramidal cell size asymmetries within auditory and language-associated regions of the temporal lobes. *Brain Lang* 86:226–242.
- Innocenti GM (1994): Some new trends in the study of the corpus callosum. *Behav Brain Res* 64:1–8.
- Jacobs B, Schall M, Scheibel AB (1993): A quantitative dendritic analysis of Wernicke's area in humans. II. Gender, hemispheric, and environmental factors. *J Comp Neurol* 327:97–111.
- Jaeger JJ, Lockwood AH, Van Valin RD, Jr., Kemmerer DL, Murphy BW, Wack DS (1998): Sex differences in brain regions activated by grammatical and reading tasks. *Neuroreport* 9:2803–2807.
- Jones DK (2004): The effect of gradient sampling schemes on measures derived from diffusion tensor MRI: a Monte Carlo study. *Magn Reson Med* 51:807–15.
- Josse G, Mazoyer B, Crivello F, Tzourio-Mazoyer N (2003): Left planum temporale: an anatomical marker of left hemispheric specialization for language comprehension. *Brain Res Cogn Brain Res* 18:1–14.
- Luders E, Rex DE, Narr KL, Woods RP, Jancke L, Thompson PM, Mazziotta JC, Toga AW (2003): Relationships between sulcal asymmetries and corpus callosum size: gender and handedness effects. *Cereb Cortex* 13:1084–1093.
- Martin RC (2003): Language processing: functional organization and neuroanatomical basis. *Annu Rev Psychol* 54:55–89.
- Moffat SD, Hampson E, Lee DH (1998): Morphology of the planum temporale and corpus callosum in left handers with evidence of left and right hemisphere speech representation. *Brain* 121:2369–2379.
- Mori S, Kaufmann WE, Davatzikos C, Stieltjes B, Amodei L, Fredrickson K, Pearlson GD, Melhem ER, Solaiyappan M, Raymond GV, Moser HW, van Zijl PC (2002): Imaging cortical association tracts in the human brain using diffusion-tensor-based axonal tracking. *Magn Reson Med* 47:215–223.
- Mori S, van Zijl PC (2002): Fiber tracking: principles and strategies—a technical review. *NMR Biomed* 15:468–480.
- Morris JA, Jordan CL, Breedlove SM (2004): Sexual differentiation of the vertebrate nervous system. *Nat Neurosci* 7:1034–1039.
- Oldfield RC (1971): The assessment and analysis of handedness: the Edinburgh inventory. *Neuropsychologia* 9:97–113.
- Parker GJ, Luzzi S, Alexander DC, Wheeler-Kingshott CA, Ciccarelli O, Lambon Ralph MA (2005): Lateralization of ventral and dorsal auditory-language pathways in the human brain. *Neuroimage* 24:656–666.
- Petrides M, Pandya DN (1988): Association fiber pathways to the frontal cortex from the superior temporal region in the rhesus monkey. *J Comp Neurol* 273:52–66.
- Pujol J, Deus J, Losilla JM, Capdevila A (1999): Cerebral lateralization of language in normal left-handed people studied by functional MRI. *Neurology* 52:1038–1043.
- Schmithorst VJ, Wilke M, Dardzinski BJ, Holland SK (2002): Correlation of white matter diffusivity and anisotropy with age during childhood and adolescence: a cross-sectional diffusion-tensor MR imaging study. *Radiology* 222:212–218.
- Seldon H (1985): Association and auditory cortices. In: Peters A, Jones EG, eds. *Cerebral Cortex*. Vol. 4. New York: Plenum Press. p 359.
- Shapleske J, Rossell SL, Woodruff PW, David AS (1999): The planum temporale: a systematic, quantitative review of its structural, functional and clinical significance. *Brain Res Brain Res Rev* 29:26–49.
- Shaywitz BA, Shaywitz SE, Pugh KR, Constable RT, Skudlarski P, Fulbright RK, Bronen RA, Fletcher JM, Shankweiler DP, Katz L, et al. (1995): Sex differences in the functional organization of the brain for language. *Nature* 373:607–609.
- Steinmetz H, Rademacher J, Huang YX, Heffer H, Zilles K, Thron A, Freund HJ (1989): Cerebral asymmetry: MR planimetry of the human planum temporale. *J Comput Assist Tomogr* 13:996–1005.
- Steinmetz H, Volkman J, Jancke L, Freund HJ (1991): Anatomical left-right asymmetry of language-related temporal cortex is different in left- and right-handers. *Ann Neurol* 29:315–319.
- Tzourio-Mazoyer N, Josse G, Crivello F, Mazoyer B (2004): Interindividual variability in the hemispheric organization for speech. *Neuroimage* 21:422–435.
- Tzourio N, Crivello F, Mellet E, Nkanga-Ngila B, Mazoyer B (1998): Functional anatomy of dominance for speech comprehension in left handers vs. right handers. *Neuroimage* 8:1–16.
- Ungerleider LG, Haxby JV (1994): “What” and “where” in the human brain. *Curr Opin Neurobiol* 4:157–165.
- von dem Hagen EA, Henkelman RM (2002): Orientational diffusion reflects fiber structure within a voxel. *Magn Reson Med* 48:454–459.
- Zaidel E, Aboitiz F, Clarke J (1995): Sexual dimorphism in interhemispheric relations: anatomical-behavioral convergence. *Biol Res* 28:27–43.